Adsorption on metal oxides: Studies with the metastable impact electron spectroscopy

S. Krischok, O. Höfft, V. Kempter *

Institut für Physik und Physikalische Technologien der Technischen Universität Clausthal, Leibnizstr. 4, 38678 Clausthal-Zellerfeld, Germany

Abstract

An overview is given on the application of metastable impact electron spectroscopy, in combination with UPS, to the study of clean magnesia and titania surfaces and their interaction with metal atoms and small molecules. The mechanisms for metal adsorption on reducible (titania) and non-reducible (magnesia) substrates are different: while on titania the metal atom often bonds by electron transfer to Ti3d states, it is hybridization of the adsorbate and anion wavefunctions which accounts for the bonding on MgO. In the case of H_2O, molecular adsorption takes place both on MgO and TiO_2; on the other hand, water-alkali coadsorption leads to hydroxide formation. In the case of CO_2, chemisorption takes place in form of carbonate (CO_3) species. These originate from the CO_2 interaction with O^{2-} surface anions. While for CaO chemisorption takes place at regular oxygen sites, for MgO this occurs at low-coordinated oxygen ions only; for TiO_2 chemisorption requires alkali coadsorption. © 2002 Elsevier Science B.V. All rights reserved.

1. Introduction

Oxides and their surface chemistry find increasing attention in surface physics [1–4]. Only during the past decade a considerable effort has been made to understand, in a systematic way, both from the point of view of theory and experiment, the properties of oxide surfaces and interfaces. They play an important role in a number of applications, as in corrosion protection, in thermal coatings, as inert supports in catalysis, and in microelectronics because of their dielectric properties; many microporous materials are based on oxides. A considerable effort is now underway to better characterize oxide surfaces and interfaces: techniques have been developed to grow, under ultrahigh vacuum (UHV) conditions, well-defined oxide films on metal supports. In this way the difficulties connected with the use of electron spectroscopic techniques for the study of insulating materials can be overcome [5]. In parallel, computational activities based on accurate first-principles calculations are well underway [2–4].

---

* Corresponding author. Tel.: +49-5323-72-2363; fax: +49-5323-72-3600.
E-mail address: volker.kempter@tu-clausthal.de (V. Kempter).

Important properties of oxide-based materials are often based on the presence of defects, point defects in particular, but also low-coordinated sites, surface vacancies, impurity atoms etc. [3,4]. These centers influence the optical, electronic, and transport properties of the material, and consequently also dominate the chemistry of its surface. A detailed understanding of their properties as well as the control of their surface concentration is therefore of considerable importance. More specifically, the regular surface sites are most likely not the best candidates where a metal cluster would start to grow during metal deposition, nor would these be the preferred sites where molecular or dissociative chemisorption of molecules, as water or CO_2, would take place. It has become clear that experiment and theory need to work together closely in order to identify and characterize the defects and the defect-induced processes and the resulting products unambiguously [1,3].

Among the electron spectroscopic tools the metastable impact electron spectroscopy (MIES) is characterized by its extremely high-surface sensitivity because the He* probe atoms interact with the edge of the surface when still 3–5 a.u. away from the surface [6,7]. Consequently, the spectral information obtained on the adsorbed species is barely disturbed by that from the underlying substrate. As far as defects are concerned, MIES can often detect them efficiently as long as they represent occupied states in the band gap. It is the aim of this report to summarize the progress made with the application of MIES, in conjunction with other surface analytical techniques, as photoelectron spectroscopy and desorption spectroscopy in particular, to oxide materials and to chemical reactions at their surfaces.

2. Experimental remarks

The experiments were carried out in UHV systems (base pressure $<2 \times 10^{-10}$ Torr) equipped with low-energy electron diffraction (LEED), temperature programmed desorption (TPD), X-ray and ultraviolet photoelectron spectroscopy (XPS and UPS), Auger electron spectroscopy (AES), and MIES; they are described elsewhere [8–11]. In

MIES metastable He*1s2s atoms are utilized to eject electrons from the surface. Since the metastables approach the surface with near-thermal kinetic energy (60–l00 meV), this technique is non-destructive and highly surface sensitive (see [6,7] for more detailed introductions in MIES and its various applications in molecular and surface spectroscopy). A discharge source serves both as the source for an intense beam of He*1s2s atoms for MIES and as a HeI photon source for UPS (HeI with 21.2 eV). The spectral contributions from metastables and photons are separated be means of a time-of-flight technique combined with a double counter system for the quasi-simultaneous aquisition of MIES and UPS spectra.

By applying a suitable bias potential between sample and spectrometer, the electrons emitted from the Fermi level, E_F, are registered at 19.8 eV (the potential energy of He*(2^3S)). In this way the energy lost by the ejected electrons in order to overcome the surface work function (WF) is compensated. Consequently, the low-energy onset of the spectra occurs at the WF of the sample. The variation of the onset of the spectra at low-kinetic energies with exposure gives then directly the exposure dependence of the surface WF.

3. Results

3.1. Oxide surfaces

For discussing the basic physics and chemistry of adsorbates on oxide surfaces a thorough understanding of the atomic and electronic structure of the clean surfaces, including information on the type and the density of eventual point and extended defects, appears indispensable [1–4].

3.1.1. Mo(100) supported MgO films

The MgO substrates used for the present study are ultrathin MgO films grown by depositing Mg in 1×10^{-6} Torr O_2 ambient on Mo(100) substrates at 550 K, followed by a 20 min annealing at 750 K in a 1×10^{-8} Torr O_2 background. The Mg source is made from a high-purity Mg ribbon wrapped around a tantalum filament. As shown in previous investigations, MgO films prepared under

these conditions grow epitaxially on the Mo(1 0 0) substrate [5]. The quality of the MgO layers is checked with MIES, UPS, AES and LEED. Even though a (1 × 1) LEED pattern is obtained from the films, the broadness of the reflexes suggests a mosaic structure of MgO domains, 50–100 nm in size [12,13].

The bottom spectrum in Fig. 1(a) is for the clean MgO film. No intensity is seen between E_F and the top of the O2p valence band (VBM). The rise of the intensity for binding energies larger than about 11.5 eV is due to scattered and secondary electrons. As explained in detail elsewhere [14–16], MIES spectra acquired from MgO surfaces essentially image the MgO(1 0 0) surface density of states (SDOS) as seen via an Auger de-excitation (AD) process. Briefly, no occupied states exist in resonance with the impinging He2s electron. Thus, no resonant tunneling of the He2s electron can occur, and the MIES spectra are due to the AD process, which in turn allows a direct comparison between MIES and UPS data [15,16]: we can expect prominent features in the SDOS, as in particular those from the O2p emission, to appear at the same binding energies in MIES and UPS.
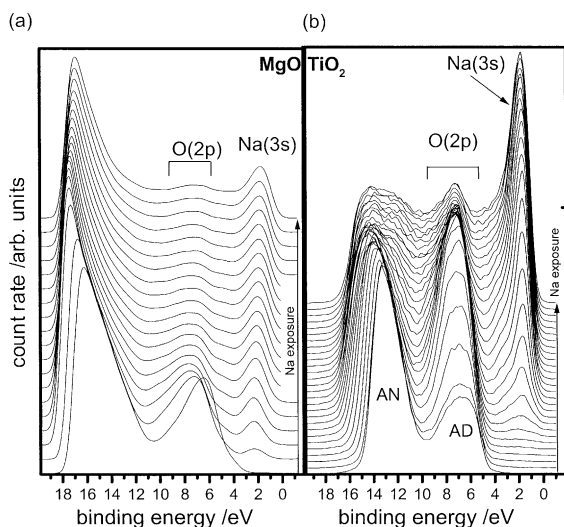

Fig. 1. MIES spectra for Na adsorption on MgO films on Mo(1 0 0) [11] (a), and TiO$_2$(1 1 0) [21] (b). In (a) the saturation coverage at room temperature is reached for spectrum nr.10 from the bottom. In (b) the relation between exposure and metal coverage is discussed in the text.

However, the selection rules for photoionization and AD are quite different, i.e. due to the exchange type interaction of the metastable atom with the surface, AD is particularly sensitive to the projected density of states in front of the surface, whereas UPS probes the average character of several top layers. Consequently, the O2p states protruding into the vacuum are seen more pronounced with MIES than with UPS.

A comprehensive overview about possible defect structures at the MgO(1 0 0) surface, their electronic structure and their influence on the surface chemistry, has recently been published [3,4]. AD spectra for the perfect and defective MgO(0 0 1) surface have been calculated in [15]. It is predicted that oxygen surplus, such as peroxides, produces additional intensity just above and below the MgO O2p substrate emission. On the other hand, anion vacancies, that is, F-type centers, should lead to a prominent feature, well separated, about 2 eV above the MgO valence band (VB). Even though the energetic location of these type of defects relative to the Fermi level of the supporting metal substrate has been calculated, due to the uncertainty of the given energy values it is not possible to clearly predict the appearance of a F-type center related feature in MIES. Recently, the thermal generation of defects in ultrathin MgO films was studied by UPS and MIES [17]. Prior to annealing, the Mo(1 0 0) supported MgO films were exposed to Li in order to promote the creation of anion vacancies. It could be shown that annealing the Li doped MgO films to 1100 K for approx. 1 min, followed by a rapid quenching to 100 K, results in a noticeable increase in intensity in the band gap region between the VBM and E_F, and this was interpreted as a signature for the presence of F-centers.

3.1.2. Titania single crystals

Prior to any study, the surface of TiO$_2$ single crystals (MATECK company) was prepared by Ar$^+$ sputtering and vacuum annealing procedures (which were different for the (1 1 0) and (1 0 0) surface), without additional oxygen treatment, in order to obtain the (1 × 1)-ordered LEED-structure for the (1 1 0) and the (1 × 3)-structure for the (1 0 0) surface [18,19].

As compared to MgO, the MIES spectrum is more complex, consisting of two parts denoted by Auger neutralization (AN) and AD (see Fig. 1(b, bottom)), both originating from the ionization of O(2p) VB states. A simulation of the spectra along the lines outlined in [20] has yielded the following picture [18]: for the studied $TiO_2(1\,1\,0)$ rutile surface E_F is located close to the conduction band minimum. Consequently, resonance ionization, followed by AN, dominates the He* interaction with the surface [6,7], leading to the AN contribution. As noted from the spectra, only a minor part of the He* species is de-excited via the AD process. However, with decreasing surface WF, induced by alkali adsorption, the contribution from AD increases strongly (see [18,19]).

Oxygen vacancies are the dominant point defect species at titania surfaces [1,3]. Differently from MgO, the electrons remaining at the surface do not localize at the site of the missing oxygen species, but rather reduce Ti-cations to $Ti^{3+}(3d)$; the corresponding spectral feature is seen in the UPS(HeI) spectra at about $E_B = 1$ eV. The spectral contribution from 3d ionization cannot be identified unambiguously in the MIES spectra: the AN contribution involving the 3d electron and one O2p electron overlaps with AD.

4. Metals on oxides

4.1. Metals on titania

The systems studied so far with MIES, in combination with UPS, include Li, Na, Mg, K, and $Cs/TiO_2(1\,1\,0$ and $1\,0\,0)$. Results for Li and $Na/TiO_2(1\,1\,0)$ can be found in [21], for K/TiO_2-$(1\,0\,0)$ and $Cs/TiO_2(1\,1\,0)$ in [18,19,22], and for $Mg/TiO_2(1\,0\,0)$ in [23]. For all studied systems, upon adsorption, the valence electron of the adsorbate is transferred to the surface and localizes at the Ti^{4+}-cation reducing it to $Ti^{3+}(3d)$. Thus, in the early stage the $Ti^{3+}(3d)$ signal seen in UPS increases. As an example, Fig. 1(b) presents MIES results for $Na/TiO_2(1\,1\,0)$ as function of the Na exposure [21]. When the minimum of the WF occurs, the Na coverage of the surface has reached

0.5 ML [21] (for details of the calibration of the exposure scale in terms of the alkali coverage, see Ref. [18]). In MIES no intensity is seen above the VBM up to E_F (see Fig. 1(b); exposures corresponding to Na coverages below about 0.25 ML); obviously, there is no charge density left at the adsorbate core. At exposures, corresponding to coverages larger than 0.3 ML, the electron transfer becomes incomplete, in this way reducing the Coulomb repulsion between adjacent adsorbate cores. This explains the strong feature seen in Fig. 1(b) near E_F at larger exposures. It originates from the transfer of adsorbate s-charge to the He* probe atom, forming a temporary He$^{-*}1s2s^2$ negative ion which decays by autodetachment. Summarizing, a fully ionic bond is formed at small exposures; however, it becomes increasingly less ionic for coverages larger than 0.3 ML.

Results of first-principles calculations exist for K [24], Cu, Ag [25]/$TiO_2(1\,1\,0)$. Indeed, upon chemisorption these adsorbates transfer their valence electrons to the cation, and form an ionic bond with a surface anion. For K/TiO_2 it is predicted that the K adsorbate is not anymore fully ionized beyond 0.5 ML coverage [24]. On the other hand, for Pd and $Au/TiO_2(1\,1\,0)$ no electron transfer from the adsorbate to the surface is predicted by first-principles calculations [24,25]. This can be explained by the fact that the weakest bound adsorbate electrons, 3d for Pd and 6s for Au, are too far off-resonance from the Ti3d level. Here the bonding is due to covalent mixing of surface and adsorbate orbitals [24,25].

4.2. Metals on MgO films

The interaction of a number of metal atoms (Na, Mg, Cu, Ag, Pd) with MgO films (see Section 3.1) was studied with MIES in combination with UPS(HeI and II) [26,27]. In all cases, except for Pd, metal-induced intensity appears between VBM and E_F. Other than for titania, the wide band gap and the location of E_F near the middle of the band gap, prevent electron transfer to the ideal MgO surface. Consequently, the valence electrons of the metal remain localized at the adsorbate, even in the early stage of exposure, and can be detected

with MIES (see Fig. 1(a)). Whether a peak-like structure or a shoulder is seen above VBM depends upon the WF of the metal/MgO combination [26]. For WF > 3.5 eV the He2s electron can be transferred into empty states at the surface, presumably localized at the adsorbate. The metal-induced intensity is then due to AN involving metal valence electrons. Indeed, this occurs for Ag and Cu/MgO [26,27], and involves two s-electrons from small metal clusters formed already in the early stage of metal adsorption. For Pd, the metal-induced emission stems from the Pd3d electrons and overlaps with the emission from O2p ionization [27].

Alkali and Mg adsorption both produce a peak right below E_F [11,28]. As discussed in Section 4.1 for titania, it is mostly due to autodetachment of He^{-*} for K, Cs and AD for Li, Na and Mg where WF is too large for efficient He^{-*} formation. Fig. 1(a) and (b) compare the evolution of the spectra for Na/MgO and Na/TiO$_2$ as a function of the Na exposure. The main difference between Na/TiO$_2$ and Na/MgO is the exposure dependence of the feature Na(3s) which originates from the presence of the 3sNa electron at the Na core: for MgO Na(3s) is seen immediately after starting the Na exposure, while for TiO$_2$ it is not seen as long as the adsorbate remains fully ionized, i.e. up to a coverage of 0.25 ML. For Mg/MgO the comparison with first principle calculations suggests that Mg atoms chemisorb covalently at extended surface defects, as steps in particular [28]. These atoms act as nucleation centers for the adsorption of additional Mg atoms. Thus, the intensity, as seen with MIES above VBM, stems from the ionization of small Mg clusters, and this part of the MIES spectra images the SDOS of these surface clusters.

First-principles calculations for metal/MgO systems suggest that at the ideal surface of MgO, quite generally, a weak covalent-type bond is formed between the metal and oxygen anions [29,30]. Results for MgO with point defects modify this picture and suggest that the strongest bonds normally involve defects [3,31]; atoms bonded in this way then act, as discussed above for Mg/MgO, as nucleation centers for the growth of metal particles and films.

5. Molecules on oxides

5.1. Interaction of carbon dioxide with alkaline earth oxides and titania

Excellent reviews exist which concentrate on the CO$_2$/metal interaction [32,33]. MIES in combination with UPS has been applied to the study of the interaction of CO$_2$ with MgO and CaO [9,10], and with bare and alkalated TiO$_2$(1 0 0) rutile [22]. The studies were carried out at room temperature. In those cases where chemisorption occurs, it takes place in form of carbonate (CO$_3$) complexes whereby the CO$_2$ adsorbates interact with surface oxygen anions. The identification of the CO$_2$-induced features follows from photoelectron spectroscopy results for CaCO$_3$ bulk samples [34], and has been discussed in detail in [9,10]. The spectral features seen in MIES and UPS can be assigned to the MOs (1a$_2'$; 1e''; 4e') (6.4 eV) and (3e'; 1a$_2''$) (11.0 eV) and (4a') (13.2 eV) of the CO$_3$ species.

However, the conditions for chemisorption differ for the studied oxides: while for MgO it takes place at surface defects only, presumably low-coordinated oxygen ions, it occurs for CaO also at regular oxygen surface sites. No CO$_2$ chemisorption at all can be detected on bare titania (not even at 130 K); carbonate formation is only seen when alkali atoms are preadsorbed [22]. On the other hand, alkali preadsorption does not have a dramatic effect for chemisorption on MgO [10].

For MgO and CaO results of first-principles calculations are available [2–4,35]. They explain the different behaviour as follows: in both cases the chemisorption mechanism is the same: charge transfer from O^{2-} to the lowest unoccupied $2\pi_u$ MO of CO$_2$ takes place. However, the (CO$_2$–O^{2-})-interaction potential along the reaction coordinate possesses a minimum for O^{2-} at regular sites only in the case of CaO; for MgO the potential displays a minimum of similar depth only for low-coordinated oxygen sites. This is explained by the fact that the O^{2-} donor level at a regular surface site of CaO and the $2\pi_u$ MO of CO$_2$ have similar energies. This greatly facilitates the electron transfer to CO$_2$. For MgO the corresponding O^{2-} donor level is at larger binding energies for regular oxygen

sites, and only the corresponding levels for oxygen at step or corner sites have comparable energetic positions as those for oxygen at regular sites for CaO. Thus, for MgO the situation at low-coordinated sites is similar to that for CaO at regular sites [2–4].

Apparently, for titania the interaction potential along the reaction coordinate possesses a barrier which prevents the formation of a $(CO_2–O^{2-})$ complex. Alkali adsorption changes the interaction potential drastically as is apparent from the increase of the sticking coefficient for CO_2 by many orders of magnitude. The MIES results show the importance of the transfer of the alkali s-electron to the CO_2: as soon as CO_2 is offered to the titania surface, precovered with alkali atoms, the spectral feature near E_F caused by the presence of the alkali s-electron at the adsorbate disappears quickly [22]. The electron transfer, presumably into the $2\pi_u$ MO, assists the formation of a bent CO_2^- species, and, as a consequence, facilitates CO_2 chemisorption as a (sp^3)-hybridized CO_3 species at surface oxygen sites.

5.2. Interaction of water with MgO and titania

Among other reasons detailed information on the water–oxide interaction is fundamental for understanding hydroxylation processes taking place in nature [36,37]. Moreover, titania is a popular electrode material in photosplitting and photooxydation devices [38]. Therefore, the water interaction with oxides and the water–oxide interface, in particular in aquous environment, has found considerable experimental and theoretical interest [1,37,38]. Even for the most-studied case, water interacting with titania, still no general agreement exists how the interface looks like. According to theory, single water molecules are predicted to adsorb dissociatively (for recent work see [39,40]); experimentally it is found that water adsorbs essentially molecularly. The identification of water-derived spectral features with photoelectron spectroscopy is difficult because OH and H_2O features overlap with emission from the titania VB and, furthermore, they cannot be separated unambiguously if both species are present at the surface simultaneously [1]. At least the former

problem can be overcome with MIES, being sensitive to the adsorbed species only.

MIES results, supplemented by HeI and II results, collected for $TiO_2(1 1 0)$ at 130 K, show that molecular adsorption dominates by far [21,41]. The situation is similar as for MgO [42,43]. An eventual dissociation at point defects cannot be excluded; the respective OH species, if present at all, do however occupy at most 5% of the available surface sites. While in UPS the intensity of the signals from molecular water depends linearly on exposure up to about 10 L, the MIES signal deviates from linearity already at 2 L. Supported by TPD results [21] we concluded that 2D-water clusters become formed above 2 L, far before the surface is fully covered by a water layer. Even for the smallest exposures we propose that the lateral interaction between adjacent water molecules by hydrogen bonding prevents their dissociation. This removes the discrepancy with theory where generally the adsorption of isolated water molecules is considered. Recent results from theory, taking into account the lateral interaction between adjacent adsorbed water species, indeed confirm its importance for the stabilization of the molecular species [40,44].

The situation changes drastically, both for MgO and TiO_2, when metal atoms (alkali or Mg) are preadsorbed: in this case water adsorbs dissociatively, even at room temperature [11,41]. Fig. 2 presents results for the interaction of water with Li/TiO_2 [41]. Upon water exposure, the peak Li(2s), signaling the presence of the valence electron at the alkali core, disappears quickly. This is indicative for charge transfer from the alkali to the water giving rise to an (alkali-OH) complex. Simultaneously, the two features 1π and 3σ, characteristic for OH formation, appear (1π coincides with the O2p valence band emission of TiO_2). The importance of the electron transfer to water is underlined by the fact that, after complete "consumption" of the alkali charge density, additional water molecules offered at 130 K are adsorbed molecularly, on top of the alkali-OH mixed layer. This is manifested by the emergence of the three structures $1b_1$, $3a_1$ and $1b_2$ from the ionization of the highest MOs of molecular water. Further support for the importance of the (alkali-water)
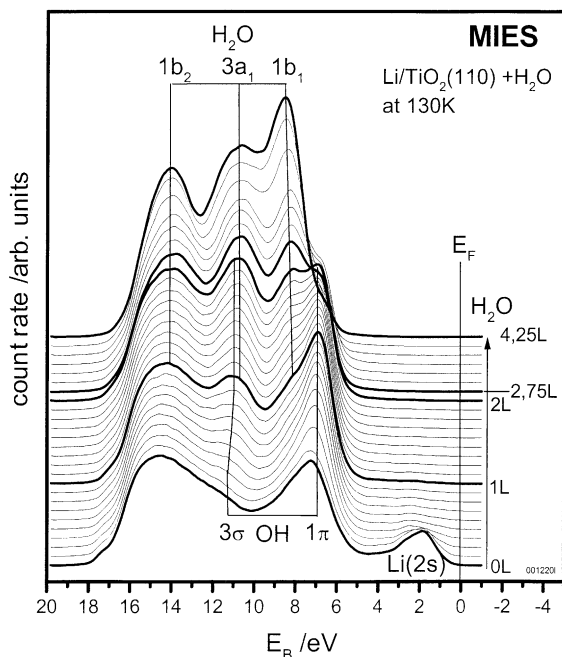
Fig. 2. MIES spectra for TiO$_2$(1 1 0), precovered with about 1 ML Li, exposed to water at around 120 K [41]. The total exposure is given in Langmuirs (L) (1 Langmuir = 10^{-6} Torr s).

charge transfer comes from the fact that water dissociation is also noted when water multilayers are exposed to alkali atoms: as a consequence hydroxyl features are seen simultaneously with those from molecular water [21].

6. Summary

MIES, combined with UPS studies dealing with the characterization of metal oxide surfaces (MgO; TiO$_2$) and the investigation of the chemistry at these surfaces are reviewed. Information is obtained on the mechanisms for metal adsorption and for molecular chemisorption. A number of important issues can now be studied in more detail, as the chemistry on water multilayers grown on oxides (which can be considered as a realistic model for films of liquid water) [11,37], the water–oxide interface in an aquous environment [43], and the interaction of organic films with oxides which is important for biomedical applications.

References

[1] V.E. Henrich, P.A. Cox, The Surface Science of Metal Oxides, Cambridge University Press, Cambridge, 1994.
[2] G. Pacchioni, Surf. Rev. Lett. 7 (2000) 277.
[3] G. Pacchioni, in: D.P. Woodruff (Ed.), The Chemical Physics of Solid Surfaces, Vol. 9, Elsevier, Amsterdam, 2000.
[4] G. Pacchioni, in: Chemisorption and Reactivity of Supported Clusters and Thin Films, Kluwer Academic Publishers, Dordrecht, 1997.
[5] M.-C. Wu, J.S. Corneille, C.A. Estrade, J.-W. He, D.W. Goodman, Chem. Phys. Lett. 182 (1991) 472.
[6] Y. Harada, S. Masuda, H. Osaki, Chem. Rev. 97 (1997) 1897.
[7] H. Morgner, Adv. Atom. Mol. Opt. Phys. 42 (2000) 387.
[8] W. Maus-Friedrichs, M. Wehrhahn, S. Dieckhoff, V. Kempter, Surf. Sci. 249 (1991) 149.
[9] D. Ochs, M. Brause, B. Braun, W. Maus-Friedrichs, V. Kempter, Surf. Sci. 397 (1998) 101.
[10] D. Ochs, B. Braun, W. Maus-Friedrichs, V. Kempter, Surf. Sci. 417 (1998) 390.
[11] J. Günster, S. Krischok, V. Kempter, D.W. Goodman, Surf. Rev. Lett. (2002), in press.
[12] M.C. Gallagher, M.S. Fyfield, J.P. Cowin, S.A. Joyce, Surf. Sci. 339 (1995) L909.
[13] C. Tegenkamp, H. Pfnür, W. Ernst, U. Malaske, J. Wollschläger, D. Peterka, K.M. Schröder, V. Zeilasek, M. Henzler, J. Phys. Cond. Mat. 11 (1999) 9943.
[14] V. Kempter, Mat. Sci. Forum 239–241 (1997) 621.
[15] L.N. Kantorovich, A.L. Shluger, P.V. Sushko, A.M. Stoneham, Surf. Sci. 444/445 (2000) 31.
[16] D. Ochs et al., Surf. Sci. 365 (1996) 557.
[17] A. Kolmakov, J. Stultz, D.W. Goodman, J. Chem. Phys. 113 (2000) 7564.
[18] M. Brause, S. Skordas, V. Kempter, Surf. Sci. 445 (2000) 224.
[19] M. Brause: Doctoral thesis, TU Clausthal, 2000.
[20] P. Eeken, J.M. Fluit, A. Niehaus, I. Urazgil'din, Surf. Sci. 273 (1992) 160.
[21] S. Krischok, Doctoral Dissertation TU Clausthal, 2001.
[22] M. Brause, V. Kempter, Surf. Sci. 476 (2001) 78.
[23] M. Brause, V. Kempter, Surf. Sci. 490 (2001) 153.
[24] T. Bredow, G. Pacchioni, Surf. Sci. 426 (1999) 106.
[25] L. Giordano, G. Pacchioni, T. Bredow, J.F. Sanz, Surf. Sci. 471 (2001) 21.
[26] P. Stracke, S. Krischok, V. Kempter, Surf. Sci. 473 (2001) 86.

S. Krischok et al. / Nucl. Instr. and Meth. in Phys. Res. B 193 (2002) 466–473

473

[27] P. Stracke, Doctoral Dissertation TU Clausthal, 2001.

[28] L.N. Kantorovich, A.L. Shluger, P.V. Sushko, J. Günster, P. Stracke, D.W. Goodman, V. Kempter, Faraday Disc. 114 (1999) 173.

[29] A. Matveev, K. Neyman, G. Pacchioni, N. Rösch, Chem. Phys. Lett. 299 (1999) 603.

[30] A. Ferrari, C. Xiao, K. Neyman, G. Pacchioni, N. Rösch, Phys. Chem. Chem. Phys. 1 (1999) 4655.

[31] A.M. Ferrari, G. Pacchioni, J. Phys. Chem. 100 (1996) 9032.

[32] F. Solymosi, J. Mol. Catal. 65 (1991) 337.

[33] H.-J. Freund, M.W. Roberts, Surf. Sci. Rep. 25 (1996) 225.

[34] E. Tegeler, N. Kosuch, G. Wiech, A. Faessler, J. Electron. Spectrosc. Relat. Phenom. 145 (1986) 145.

[35] G. Pacchioni, J.M. Ricart, F. Illas, J. Am. Chem. Soc. 116 (1994) 10152.

[36] P.A. Thiel, T.E. Madey, Sur. Sci. Rep. 7 (1987) 211.

[37] G.E. Brown Jr. et al., Chem. Rev. 99 (1999) 77.

[38] A. Linsebigler, G. Lu, J.T. Yates, Chem. Rev. 95 (1995) 735.

[39] E.V. Stefanovich, T.N. Truong, Chem. Phys. Lett. 299 (1999) 623.

[40] P.J.D. Lindan, J. Muscat, S. Bates, N.M. Harrison, M. Gillan, Faraday Discuss. 106 (1997) 135.

[41] S. Krischok, O. Höfft, J. Günster, J. Stultz, D.W. Goodman, V. Kempter, Surf. Sci. 495 (2001) 8.

[42] J. Günster, G. Liu, J. Stultz, D.W. Goodman, J. Chem. Phys. 110 (1999) 2558.

[43] M.A. Johnson, E.V. Stefanovich, T.N. Truong, J. Günster, D.W. Goodman, J. Phys. Chem. B 103 (1999) 3391.

[44] D. Vogtenhuber, R. Podloucky, private communication.